Microtubules regulate GEF-H1 in response to extracellular matrix stiffness

Jessica N. Heck[a,b,c], Suzanne M. Ponik[a,c,d], Maria G. Garcia-Mendoza[a,c,e], Carolyn A. Pehlke[a,c,d,f], David R. Inman[a,c,d], Kevin W. Eliceiri[c,d,f], and Patricia J. Keely[a,b,c,d,e,f]
[a]Department of Cell and Regenerative Biology, [b]Molecular and Cellular Pharmacology Program, [c]University of Wisconsin Paul P. Carbone Comprehensive Cancer Center, [d]Laboratory for Optical and Computational Instrumentation, [e]Cellular and Molecular Biology Program, and [f]Biomedical Engineering Program, University of Wisconsin, Madison, WI 53706

ABSTRACT Breast epithelial cells sense the stiffness of the extracellular matrix through Rho-mediated contractility. In turn, matrix stiffness regulates RhoA activity. However, the upstream signaling mechanisms are poorly defined. Here we demonstrate that the Rho exchange factor GEF-H1 mediates RhoA activation in response to extracellular matrix stiffness. We demonstrate the novel finding that microtubule stability is diminished by a stiff three-dimensional (3D) extracellular matrix, which leads to the activation of GEF-H1. Surprisingly, activation of the mitogen-activated protein kinase kinase/extracellular signal-regulated kinase pathway did not contribute to stiffness-induced GEF-H1 activation. Loss of GEF-H1 decreases cell contraction of and invasion through 3D matrices. These data support a model in which matrix stiffness regulates RhoA through microtubule destabilization and the subsequent release and activation of GEF-H1.

INTRODUCTION

Increased mammographic density of breast tissue is correlated with a fourfold to sixfold increased risk of developing breast carcinoma (Boyd et al., 1998). Moreover, tumors predominantly arise in locally dense regions of the breast that are collagen rich (Ursin et al., 2005), which suggests that it is changes in the composition of the local environment that actually present the risk factor for developing breast cancer. The molecular mechanisms by which density promotes tumor formation are largely unknown.

Increased breast tissue density corresponds to increased deposition of extracellular matrix proteins, especially type I collagen (Guo et al., 2001). Breast density can be modeled in vitro using three-dimensional (3D) collagen gels of varying type I collagen con-

centrations (Wozniak and Keely, 2005). As collagen concentration is increased, the stiffness of the matrix increases (Roeder et al., 2002; Paszek and Weaver, 2004; Provenzano et al., 2009). Breast epithelial cells cultured in stiff collagen matrices have significantly increased RhoA activity compared with cells cultured in compliant collagen gels (Wozniak et al., 2003; Provenzano et al., 2009). The upstream RhoA regulatory molecules that modulate this response to changes in matrix stiffness have yet to be identified.

Previous work from our group compared the gene expression of normal mammary cells cultured in compliant and stiff collagen matrices by microarray analysis. Several mRNAs related to RhoA regulation were altered with increased matrix stiffness, including expression of Arhgef2, which encodes the protein GEF-H1 (Provenzano et al., 2009). In addition, Arhgef2/GEF-H1 was one of only two Rho guanine nucleotide exchange factors (GEFs) that were down-regulated in mammary tumors in which focal adhesion kinase (FAK) had been knocked out (Provenzano et al., 2008), further suggesting a link between this GEF and the response to the extracellular matrix. GEF-H1 was further of interest to us because of its previously reported role in mechanosignal transduction in fibroblasts (Guilluy et al., 2011) and endothelial cells (Birukova et al., 2010).

Several means of GEF-H1 regulation have been suggested. GEF-H1 binds to and is held inactive via its association with microtubules; however, with increased microtubule instability and

depolymerization, GEF-H1 is released from microtubules and is free to activate Rho (Birkenfeld *et al.*, 2008). In addition, GEF-H1 directly interacts with a variety of other protein partners (Aijaz *et al.*, 2005; Guillemot *et al.*, 2008; Nie *et al.*, 2009; Tonami *et al.*, 2011) and is highly phosphorylated, including downstream of active extracellular signal-regulated kinase and p21-activated kinase (Benais-Pont *et al.*, 2003; Zenke *et al.*, 2004; Callow *et al.*, 2005; Birkenfeld *et al.*, 2007; Fujishiro *et al.*, 2008; Waheed *et al.*, 2010), which suggests that a diverse set of signaling pathways may work synergistically with microtubules to regulate GEF-H1 activity.

On the basis of these findings, we investigated the role of GEF-H1 in regulating RhoA activity in response to 3D collagen matrix stiffness. Here we report that in breast epithelial cells, GEF-H1 exchange activity for RhoA was regulated by 3D collagen matrix stiffness. GEF-H1 was required for RhoA activation and intracellular actin/myosin contractility in response to increased matrix stiffness. Loss of GEF-H1 expression disrupted cell migration and invasion in 3D matrices. Of particular interest, microtubules were responsive to biomechanical changes of the 3D matrix environment and were part of the mechanism for GEF-H1 activation of Rho. These data demonstrate that microtubules, GEF-H1, and RhoA function together in mechanosensing, which allows breast epithelial cells to detect and respond to biomechanical changes in their tissue microenvironment.
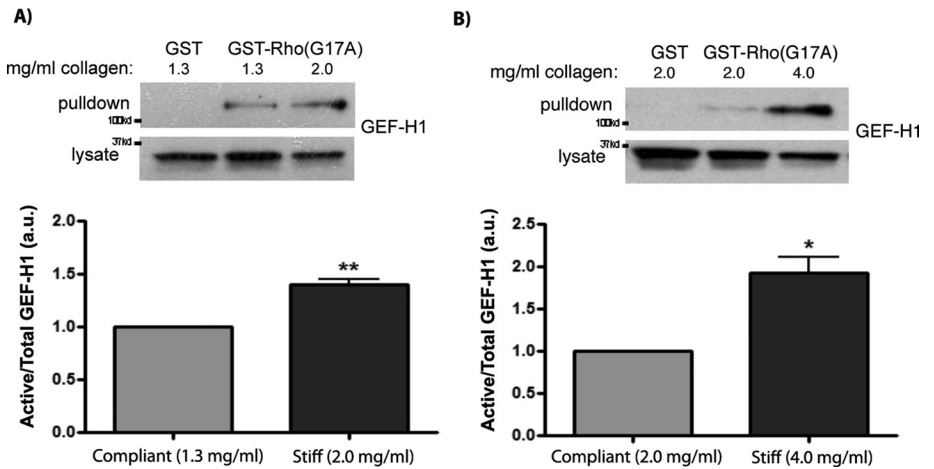

FIGURE 1: Endogenous GEF-H1 activity is regulated by extracellular matrix stiffness. (A) T47D human breast carcinoma cells were cultured in compliant (1.3 mg/ml) and stiff (2.0 mg/ml) collagen gels, and (B) normal murine mammary gland (NMuMG) cells were cultured in compliant (2.0 mg/ml) and stiff (4.0 mg/ml) collagen gels for 2 h, and then cells in collagen gels were lysed. Activated GEF-H1 was isolated by pull-down using purified GST-Rho(G17A), and the amount of GEF-H1 that was pulled down and the total amount in the lysates were determined by Western blot with anti-GEF-H1 antibodies (top). Results from four experiments were quantified and normalized to total GEF-H1 (bar graphs). In T47D cells there was an ∼40% increase in GEF-H1 activation with increased matrix stiffness; n = 4 and **p < 0.001. Similarly, in NMuMG cells there was a nearly twofold increase in GEF-H1 activity in response to increased matrix stiffness; n = 4 and *p < 0.05.

RESULTS

Endogenous GEF-H1 activity is regulated by extracellular matrix stiffness

Activated Rho GEFs have a significantly higher affinity for the nucleotide-free state of Rho than for either GTP- or GDP-bound Rho (Garcia-Mata *et al.*, 2006). This aspect can be exploited to isolate activated Rho GEFs, which can be pulled down using glutathione *S*-transferase (GST)–RhoA (G17A), a point mutation that mimics the Rho nucleotide-free state and was previously used to bind activated Rho GEFs (Garcia-Mata *et al.*, 2006; Dubash *et al.*, 2007).

To determine whether GEF-H1 exchange activity for RhoA is regulated by 3D matrix stiffness, we cultured T47D and normal murine mammary gland (NMuMG) cells in compliant and stiff collagen gels for 2 h. We previously demonstrated that increasing the concentration of collagen in 3D gels increases the elastic modulus, creating gels that are stiffer (Provenzano *et al.*, 2009). We found that different cells experience elastic modulus differently, and thus the concentration that is "stiff" or "compliant" needs to be determined empirically. Thus, for these studies, we defined a stiff matrix (high density) experimentally for each individual cell line as the concentration of collagen that cannot be contracted >10%, whereas a compliant matrix (low density) is the concentration of collagen that a particular cell line can contract at least 40%. For the highly contractile NMuMG cells, we used 2 mg/ml collagen as compliant and 4 mg/ml collagen as stiff, whereas for the less contractile T47D human breast carcinoma cell line, we used 1.3 mg/ml collagen as compliant and 2 mg/ml collagen as stiff. Using the GST-Rho(17A) pull-down assay,

we determined that the amount of activated GEF-H1 was significantly increased in stiff compared with compliant collagen gels in both T47D and NMuMG cells (Figure 1, A and B), demonstrating that GEF-H1 exchange activity for RhoA is regulated by 3D collagen matrix stiffness.

To determine whether GEF-H1 regulates RhoA downstream of matrix stiffness, stable and transient GEF-H1 knockdown cells were generated. NMuMGs were infected with vector control–pGIPz or GEF-H1 short hairpin RNA (shRNA) #1 or stably transfected with vector control-pLK0.1 or GEF-H1 shRNA #2. In addition, T47D cells were stably transfected with anti–human GEF-H1 shRNA or control nontargeting shRNA. Knockdown was determined by Western blot (Figure 2A and Supplemental Figure S1). Although GEF-H1 is implicated in mitosis (Krendel *et al.*, 2002; Bakal *et al.*, 2005; Birkenfeld *et al.*, 2007, 2008), there was no observable mitotic effect (unpublished data), nor was there any difference in cell proliferation on cells with stable GEF-H1 knockdown when cultured in collagen gels (Supplemental Figure S2). However, the stable cell lines did retain some GEF-H1 expression, which may allow them to continue through mitosis.

Consistent with previous data (Wozniak *et al.*, 2003), in shRNA control cells, the amount of active, GTP-bound RhoA was increased in stiff compared with compliant collagen gels (Figure 2B and Supplemental Figure S1). However, in cells in which GEF-H1 was knocked down, this typical increase in RhoA activity in response to increased matrix stiffness was lost (Figure 2B and Supplemental Figure S1). Of interest, with NMuMG cells that were stably transfected, we noted a slight increase in RhoA activity under compliant matrix conditions when GEF-H1 was knocked down compared with control cells. This suggests that there may be additional regulatory mechanisms that are opposed by GEF-H1 in the absence of a stimulus, a finding that is consistent with results in which GEF-H1 knockdown affects the resting state of RhoA activity in studies of growth factor stimulation (Tsapara *et al.*, 2010).
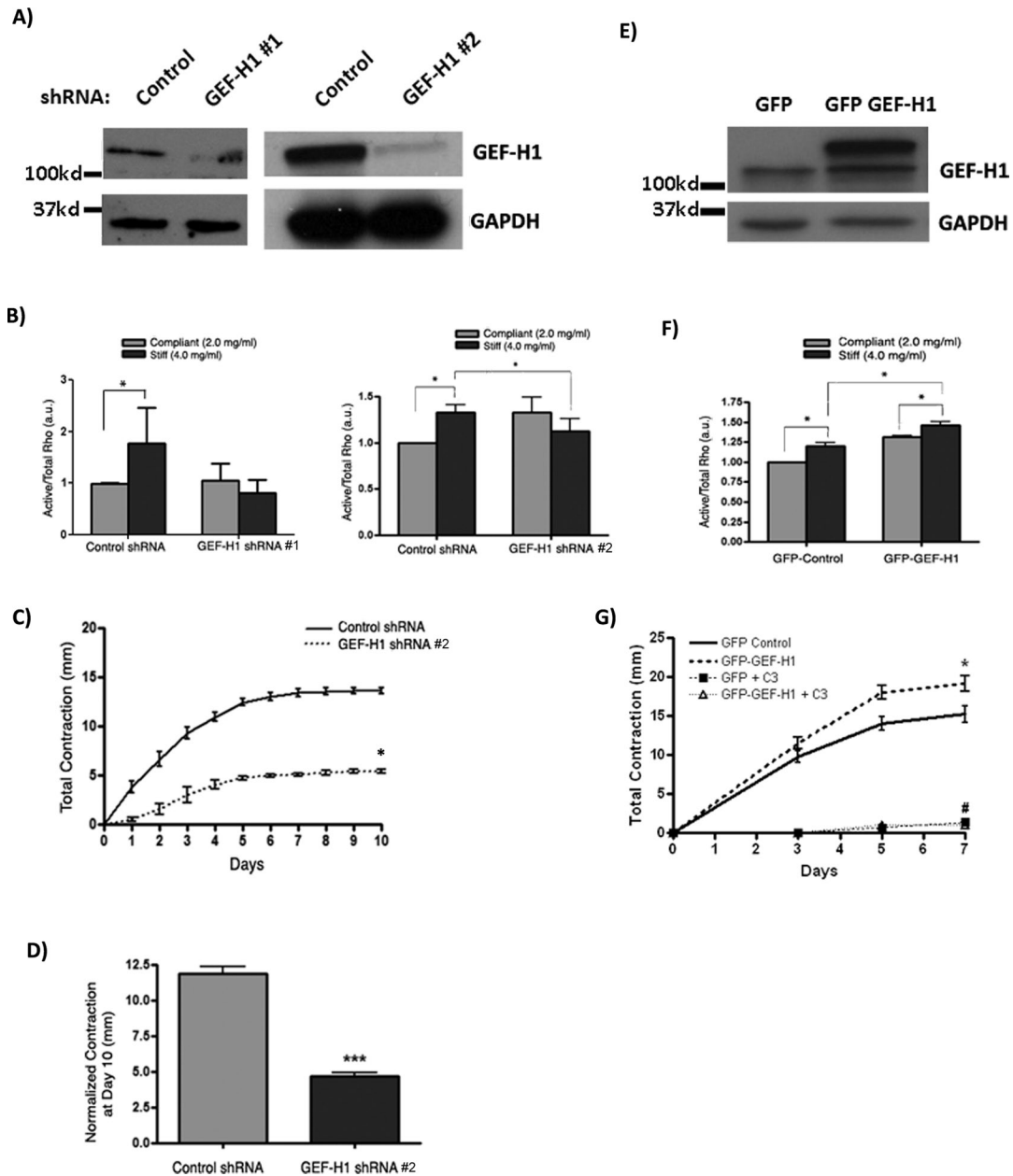
FIGURE 2: GEF-H1 is required for proper RhoA regulation and Rho-mediated actin–myosin contractility in normal murine mammary gland cells. (A) NMuMG cells were transiently infected with vector control (pGIPz) or mouse-specific GEF-H1 shRNA #1 or stably transfected with vector control (pLK0.1) or mouse-specific GEF-H1 shRNA #2. (B) Control and GEF-H1–knockdown cells were cultured in compliant and stiff collagen gels, and the amount of active RhoA (GTP bound) was measured after 2 h and normalized to total Rho. RhoA activity was increased with increased matrix stiffness; however, loss of GEF-H1 significantly disrupted proper RhoA regulation and its activation in response to increased matrix stiffness (shRNA#1, n = 3; and shRNA #2, n = 5; *p < 0.05. (C) Stable control and GEF-H1–knockdown (shRNA #2) cells were cultured in compliant collagen gels for 10 d, and the area of the collagen gel was measured daily. The resulting contraction curve demonstrates that GEF-H1–knockdown cells contracted the matrix twofold less compared with control cells over 10 d; n = 6. (D) Contractility measurements were normalized to total cellular protein on day 10 and demonstrate that the decrease in cell contraction is not due to fewer cells when GEF-H1 shRNA #2 was stably expressed; n = 6 and ***p < 0.001. (E) NMuMG cells were stably transfected with GFP vector control or GFP-GEF-H1. Note the additional, larger GEF-H1 immunoreactive band representing GFP-GEF-H1 in the transfectants. (F) GFP vector control and GFP-GEF-H1–expressing cells were cultured in compliant and stiff collagen gels, and the amount of active RhoA (GTP-bound) was measured after 2 h and normalized to total RhoA. RhoA activity was increased with increased matrix stiffness in GFP vector control cells. GFP-GEF-H1 overexpression increased RhoA activity compared with GFP vector control cells, and this activation was up-regulated further in response to matrix stiffness. n = 4 and *p < 0.05. (G) GFP vector control and GFP-GEF-H1 cells were cultured in compliant collagen gels with or without exoenzyme C3 for 7 d, and contractility was measured on days 0, 3, 5, and 7. The resulting contraction curve demonstrates that GFP-GEF-H1 overexpression increased cellular contractility compared with GFP control cells on day 7, and inhibition of RhoA blocks gel contraction in both control and GEF-H1xoverexpressing cells; n = 3; *p < 0.05 and **p < 0.0001.

Moreover, GEF-H1–knockdown cells contracted a compliant 3D collagen matrix more than twofold less compared with shRNA control cells (Figure 2, C and D). The inability of cells expressing GEF-H1 shRNA to contract the matrix is interesting, as RhoA activity was slightly elevated in compliant matrices upon GEF-H1 knockdown. However, these data are consistent with the results of Tsapara *et al.* (2010) in which expression of a dominant-negative GEF-H1 significantly reduced contractility on compliant 2D surfaces.

As a converse approach, green fluorescent protein (GFP)–tagged GEF-H1 was overexpressed in NMuMG cells (Figure 2E). Overexpression of GEF-H1 resulted in an overall increase in the amount of active, GTP-bound RhoA in both compliant and stiff matrices (Figure 2F). Furthermore, GFP-GEF-H1–overexpressing cells contracted a compliant 3D collagen matrix significantly more than GFP control cells. To validate that the effect of increased GEF-H1 was through Rho, cells were treated with cell-permeable exoenzyme C3, a nonreversible inhibitor of Rho. Collagen gel contractility in control GFP and GFP-GEF-H1–overexpressing cells was inhibited by treatment with exoenzyme C3 (Figure 2G). Combined, these data demonstrate that GEF-H1 regulates matrix contractility through regulation of RhoA.

Microtubule stability regulates GEF-H1 in response to 3D matrix stiffness

It has been demonstrated that GEF-H1 is regulated by microtubules, such that it is held inactive by binding to polymerized microtubules and is released and is free to regulate Rho under conditions of microtubule instability and subsequent depolymerization (Birkenfeld *et al.*, 2008). To explore the possibility that microtubule stability is responsive to changes in 3D matrix stiffness as a potential mechanism for GEF-H1 activation, we cultured NMuMG cells in compliant and stiff collagen gels and treated them with vehicle control, paclitaxel to stabilize microtubules, or nocodazole to depolymerize microtubules. Changes in microtubules and actin organization, as well as endogenous GEF-H1 localization (unpublished data), in response to matrix stiffness were visualized by immunofluorescence. Using acetylated tubulin as a marker for microtubule stability, we observed in both compliant and stiff collagen gels that paclitaxel increased the amount of acetylated microtubules compared with vehicle control, whereas nocodazole decreased the presence of acetylated microtubules (Figure 3A). These treatments thus served as benchmarks for increased and decreased microtubule stability. Of importance, there was a striking difference in acetylated tubulin levels in NMuMG cells that were cultured in stiff compared with compliant collagen gels: in compliant 3D matrix conditions, the acetylated microtubules appeared more linear and organized, whereas in stiff matrices acetylated microtubules were more punctate and disorganized (Figure 3, A and B). Quantification of the structural differences in acetylated microtubules of cells cultured in stiff and compliant 3D collagen gels was done using a curvelet-based analysis program, CurveAlign (www.loci.wisc.edu/software/curvelet-based-alignment-analysis), which outputs a normalized measure of anisotropy based on the distribution of curvelet coefficients (Candès *et al.*, 2006) generated from each image. This analysis demonstrated that the punctate and disorganized structures found in the cells grown in stiff collagen gels produced a more isotropic distribution of curvelet coefficients, whereas the linear and organized structures found in cells cultured in compliant collagen gels resulted in a distribution with a more distinct directionality or anisotropy (Figure 3B). Western blot analysis of acetylated- tubulin levels confirmed an increase in acetylated tubulin in compliant compared with stiff collagen gels (Figure 3C). This suggests that the changes in microtubule stability may be at least part of the mechanism for GEF-H1 regulation in response to changes in 3D matrix stiffness. Of interest, there was no obvious change in the overall structure of cortical actin organization between stiff and compliant 3D collagen matrices with or without any treatment. However, this assessment may have missed subtler differences and did not assess the actin in protrusive structures, which have been shown to differ between stiff and compliant collagen matrices (Wozniak *et al.*, 2003).

When cells cultured in compliant and stiff 3D collagen gels were treated with nocodazole, which induces microtubule depolymerization, the regulated activation of GEF-H1 in response to matrix stiffness was lost, and there was a significant increase in GEF-H1 activity in compliant matrices, nearly matching GEF-H1 activation in stiff 3D collagen gels (Figure 3D). The fact that GEF-H1 activity did not further increase in stiff matrices in response to nocodazole treatment may indicate that the activation of GEF-H1 is already maximal under these conditions, perhaps because of the minimal acetylated microtubules that are present when cells are in stiff matrices (Figure 3A). In contrast, when cells cultured in compliant and stiff matrices were treated with paclitaxel to inhibit microtubule disassembly and thus enhance microtubule stability, there was significantly less GEF-H1 activation in stiff 3D collagen gels compared with control treatment (Figure 3D). These data suggest that microtubule disassembly and dynamic instability are a critical component of GEF-H1 activation and its regulation in response to matrix stiffness.

Extracellular signal-regulated kinase 1/2 is not required for GEF-H1 activation in response to 3D matrix stiffness

In addition to microtubules, GEF-H1 activity can be regulated downstream of extracellular signal-regulated kinase (ERK) 1/2, which directly phosphorylates GEF-H1, increasing its exchange activity for RhoA in 2D culture (Fujishiro *et al.*, 2008). NMuMG cells were cultured in compliant and stiff collagen gels treated with vehicle control or the mitogen-activated protein kinase (MAPK) kinase (MEK) inhibitor UO126 to disrupt downstream signaling through ERK1/2, and then GEF-H1 activation was measured in each condition. GEF-H1 activation was increased in stiff compared with compliant 3D collagen gels after control treatment, and this was unchanged when UO126 was used to block MEK/ERK signaling (Figure 4A). In addition, there was no change in the activation of RhoA itself with increased matrix stiffness when comparing control treatment and treatment with MEK inhibitor (Figure 4B). These data were unexpected because we had previously linked matrix stiffness to ERK activation (Provenzano *et al.*, 2009), but they demonstrate that ERK1/2 regulation of GEF-H1 is not required for GEF-H1 activation or downstream RhoA activity in response to 3D matrix stiffness in epithelial cells.

GEF-H1 is required for 3D cell migration and invasion in vitro

GEF-H1 is increased in migratory cells and has been shown to regulate 2D cell migration (Nalbant *et al.*, 2009; Heasman *et al.*, 2010; Tsapara *et al.*, 2010). NMuMG cells expressing control and GEF-H1 shRNA were cultured in compliant and stiff collagen gels in a Transwell invasion assay. Knockdown of GEF-H1 expression disrupted the ability of cells to migrate through and invade the collagen gel in compliant gels compared with vector control cells (Figure 5A). We found that both control and GEF-H1 knockdown cells migrated significantly less in stiff compared with compliant collagen matrices, which may be due to an increase in the physical resistance encountered by the cell or an increase in the randomness of the migration at the expense of crossing the Transwell. We validated that this difference was not due to an effect on cell proliferation between
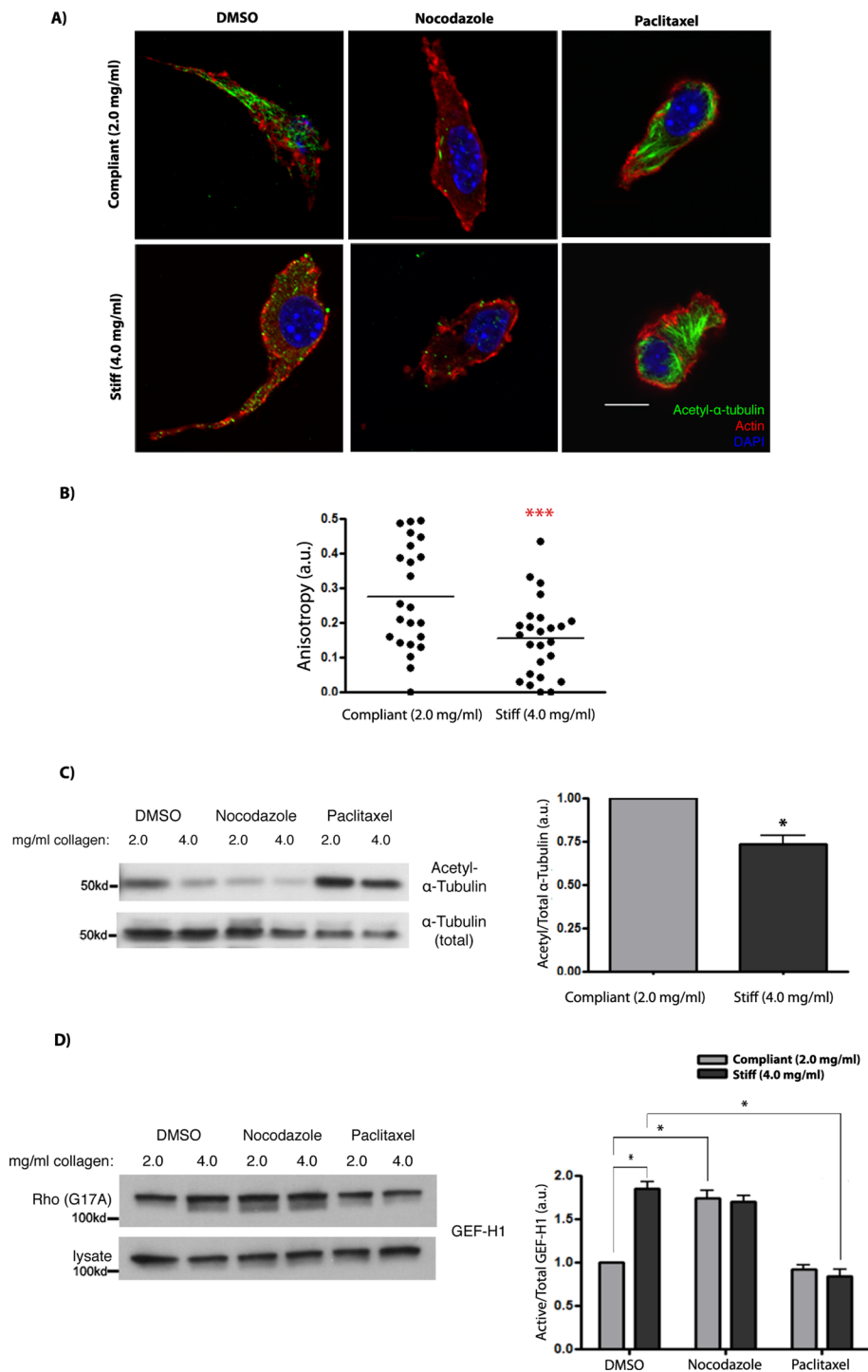
FIGURE 3: Microtubule stability is responsive to matrix stiffness and regulates GEF-H1 activity. (A) NMuMG cells cultured in compliant and stiff collagen gels were pretreated with vehicle control, 10 µM nocodazole, or 10 µM paclitaxel for 30 min, and then gels were floated in the presence of each treatment for an additional 2 h. Collagen gels were fixed in paraformaldehyde and stained for acetylated α-tubulin as a marker for stable microtubules (green) and total actin (red). Nocodazole and paclitaxel treatment resulted in clear differences in the structure of acetylated (stable) microtubules; however, there was no discernible change in actin. In contrast, there was a dramatic change in the structure of acetylated (stable) microtubules in stiff compared with compliant matrix conditions with vehicle (DMSO) treatment. (B) Acetylated (stable) microtubule structural morphology was quantified using CurveAlign software as a measure of anisotropy (increased organization of the microtubules) from 47 cells stained as in A. Each dot represents a data point, and the average value is represented by a horizontal line; n = 47 and ***p < 0.005. See *Materials and Methods* for details. (C) Cell lysates from NMuMG cells cultured in compliant and stiff collagen gels treated as described were probed for

NMuMG shRNA control and GEF-H1 knock-down cells when cultured in compliant or stiff 3D matrices (Supplemental Figure S2). To determine whether GEF-H1 plays a role in a carcinoma cell, we stably transfected the more invasive MDA-MB-231 human breast carcinoma cell line with either shRNA control or GEF-H1 specific shRNA #5. The knockdown determined by Western blot was comparable to T47D and NMuMG cells, and no effect on cell proliferation was noted (Supplemental Figure S2). Highly invasive MDA-MB-231 breast carcinoma cells also required GEF-H1 and RhoA for cell migration and invasion (Figure 5B). Again, invasion through a dense gel was less than through a compliant gel, but knockdown of GEF-H1 did significantly inhibit invasion of MDA-MB-231 cells through stiff gels.

DISCUSSION

Although previous work established that RhoA is activated by stiff collagen matrices (Wozniak *et al.*, 2003), little is known about signaling events upstream of RhoA that regulate its activity in response to increased 3D matrix stiffness. Here we report that GEF-H1 is activated by stiff collagen matrices and that GEF-H1 exchange activity is required for RhoA activation in response to extracellular matrix stiffness. In addition, these data demonstrate the unique finding that microtubule stability is responsive to changes in 3D

acetylated α-tubulin as a marker for microtubule stability and normalized to total α-tubulin by Western blot. The change in stability measured by acetylation was quantified for DMSO-treated cells (bar graph) and demonstrate that there was a significant decrease in acetylated α-tubulin, indicating a decrease in stable microtubules in stiff compared with compliant matrices; n = 3 and *p < 0.05. (D) NMuMG cells cultured in compliant and stiff collagen gels were pretreated with vehicle control (DMSO), 10 µM nocodazole, or 10 µM paclitaxel for 30 min, and then the gels were floated in the presence of DMSO or drug for an additional 2 h. The amount of activated GEF-H1 was determined by GST-Rho(G17A) pull-down and was normalized to total GEF-H1 by Western blot. There was a significant increase in GEF-H1 activity with increased stiffness; however, changes in microtubule stability via treatment with nocodazole and paclitaxel disrupted GEF-H1 regulation by matrix stiffness. Nocodazole treatment appeared to maximally activate GEF-H1 in both compliant and stiff matrix conditions, whereas treatment with paclitaxel prevented GEF-H1 activation in response to increased matrix stiffness compared with controls; n = 5 and *p < 0.05.
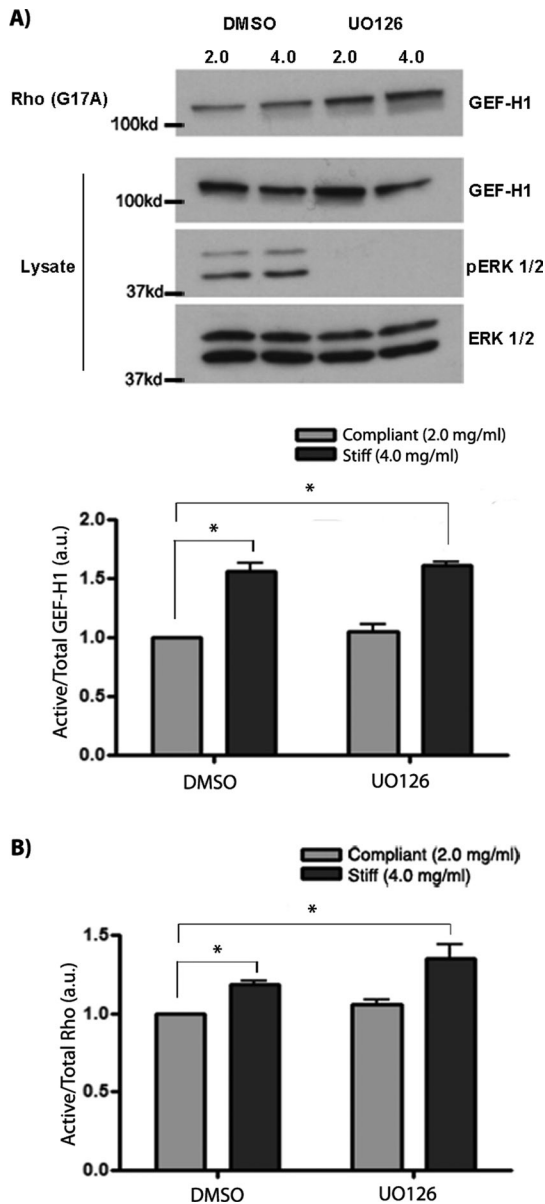
FIGURE 4: ERK1/2 signaling is not required for GEF-H1 regulation and downstream signaling in response to matrix stiffness. (A) Untransfected NMuMG cells cultured in compliant and stiff collagen gels were pretreated with vehicle (DMSO) or 10 μM UO126 for 30 min and then floated in the presence of DMSO or drug for an additional 2 h. The amount of activated GEF-H1 was determined by Rho(G17A) pull-down and was normalized to total GEF-H1 by Western blot. Treatment with UO126 did not inhibit the activation of GEF-H1 by matrix stiffness; n = 4 and *p < 0.05 (bar graph). Western blots were also probed for pERK1/2 and total ERK1/2 to verify that the U0126 inhibited phosphorylation of ERK as expected. (B) NMuMG cells were cultured as described, and the amount of active (GTP-bound) RhoA was measured after 2 h and normalized to total Rho. RhoA activity was significantly increased with increased matrix stiffness in vehicle control and UO126 treatment, which suggests that its regulation did not occur downstream of MEK and ERK1/2; n = 6 and *p < 0.05.

matrix stiffness, which in turn regulates GEF-H1 activation. Thus we propose a novel signaling pathway by which a stiff 3D matrix diminishes microtubule stability, which releases GEF-H1 in order to activate Rho.

The finding that microtubule stability is decreased with increased 3D matrix stiffness adds to a handful of observations that suggest a role for microtubules in mechanosensing. Using acetylated tubulin as a marker for microtubule stability, we find a decrease in stable microtubules in breast epithelial cells when cultured in stiff compared with compliant matrix conditions. Recent results tracking microtubules dynamically in endothelial cells demonstrate an increase in microtubule growth persistence on 2D compliant collagen-coated surfaces compared with stiff collagen-coated surfaces (Myers et al., 2011). However, in the study by Myers et al. (2011), 3D collagen matrices caused the cells to become insensitive in microtubule growth persistence, which is in contrast to our findings that mammary epithelial cells do have altered acetylated microtubules in compliant compared with stiff 3D matrices. The differences may relate to the cell type or the different methods used to assess microtubule stability, as here we used an antibody to acetylated tubulin, which is not as sensitive to dynamics as that reported by Myers et al. (2011). Moreover, our data are consistent with the finding that fibroblasts in relaxed 3D collagen gels form dendritic, microtubule-based protrusions, in contrast to actin-based lamellipodia formed on 2D collagen surfaces (Rhee et al., 2007).

Of interest, these data are in agreement with the hypothesis that actin–myosin contractility generates tension within the cell that is balanced by the microtubules resisting the resulting compression forces and by the cell attachment points to the extracellular matrix (Ingber, 2003). Consistent with results in adherent smooth muscle cells, when microtubule stability is compromised by drug treatment or in response to experimental conditions, the cell will adjust its tensile load to exert more force on the substrate in order to balance the force that can no longer be absorbed by the microtubules (Stamenovic et al., 2002). Our data are consistent with a model in which the intracellular contractile force is resisted by a stiff matrix, which relieves the compressive force that is normally absorbed by microtubules in compliant conditions.

The down-regulation of microtubule stability by increased matrix stiffness is mechanistically important, as one of the primary modes of GEF-H1 regulation is through its association with microtubules. GEF-H1 is held inactive via its association with microtubules. However, with increased microtubule instability and depolymerization resulting from upstream signaling events or artificial manipulation via drug treatment, GEF-H1 is released from microtubules and is free to activate Rho (Ren et al., 1998; Birkenfeld et al., 2008). Thus the regulated release of GEF-H1 from microtubules is an important mechanism for localized activation of Rho. In HeLa cells and fibroblasts, microtubule disassembly as a result of nocodazole treatment induces GEF-H1 activation as well as actin–myosin contractility downstream of Rho, which suggests that GEF-H1 is a potent mediator of cross-talk between microtubules and the actin cytoskeleton (Liu et al., 1998; Krendel et al., 2002; Chang et al., 2008). Although this has been explored extensively in 2D culture, microtubule regulation of GEF-H1 function has not been investigated in response to changes in 3D matrix stiffness. The data presented here are consistent with previous reports in 2D culture. These data are especially interesting, as microtubule stability has been previously been linked to patient prognosis for breast cancer (Mialhe et al., 2001).

Several observations demonstrate that microtubule tip complexes are in very close proximity to sites of cell adhesion and target RhoA activity for focal adhesion formation (Putnam et al., 2003; Small and Kaverina, 2003). Kaverina et al. (2002) found that mechanosensory signals increase microtubule polymerization and guidance of microtubules toward adhesion sites under increased tensile stress, likely through a molecular tip complex. In these
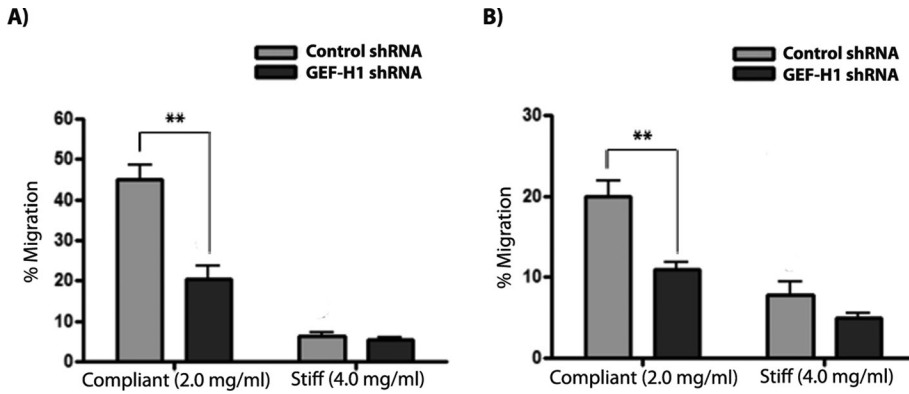
FIGURE 5: GEF-H1 expression is required for cell invasion across 3D matrices. (A) NMuMG and (B) MDA-MB-231 cells that were stably transfected with control shRNA or species-specific shRNA #5 targeting GEF-H1 were cultured within compliant and stiff collagen gels layered on top of a permeable membrane support and allowed to invade across the gel for 24 h (NMuMG) or 48 h (MDA-MB-231). Cell migration and invasion were quantified by Calcein AM live-cell staining of cells that transversed the membrane and normalized to the initial cell number. In both NMuMG and MDA-MB-231 cells, cell invasion through compliant matrices was significantly disrupted upon loss of GEF-H1 protein expression. n = 3 for each cell type and *p < 0.05. Cell invasion through stiff matrices was diminished compared with compliant matrices and may reflect either difficulties in traversing the denser matrix or a loss of persistent cell invasion toward the membrane.

studies, the mechanism linking microtubules to RhoA was not identified. Because GEF-H1 mediates the cross-talk between microtubules and the actin cytoskeleton (Krendel et al., 2002), several studies speculated on the possibility that GEF-H1 may mediate these effects at focal adhesions (Palazzo and Gundersen, 2002; Small and Kaverina, 2003).

Previous work by our lab and others demonstrates that phosphorylation of ERK1/2 is increased in stiff collagen matrices (Paszek and Weaver, 2004; Provenzano et al., 2009). These findings and the fact that GEF-H1 is directly phosphorylated by ERK1/2 (Fujishiro et al., 2008) prompted us to explore whether MAPK signaling regulates GEF-H1 and subsequently RhoA in response to extracellular matrix stiffness. Surprisingly, however, our data demonstrate that ERK1/2 does not play a significant role in GEF-H1 activation in stiff collagen matrices, as disruption of MEK/ERK signaling had no effect on GEF-H1 activation or RhoA activity in response to increased matrix stiffness. This suggests that ERK1/2 activation of GEF-H1 and GEF-H1 regulation via microtubules are likely distinct mechanisms in epithelial cells and may even be cell type specific. These results are in contrast to those of Guilluy et al. (2011), in which it was demonstrated that in fibroblasts mechanical activation of GEF-H1 occurs downstream of ERK1/2 but not downstream of microtubules. In addition to a different cell lineage, their results were based on mechanical force applied locally to beads bound via integrins to the dorsal surface of cells (Guilluy et al., 2011). These data are intriguing and beg for additional insight into cellular mechanisms used to respond to different types of forces a cell may encounter. Although data presented here do not rule out transcriptional regulation of GEF-H1 by ERK1/2 in response to matrix stiffness, in previous studies we found that regulation of GEF-H1 mRNA expression by matrix stiffness was not reversed by inhibition of the MEK/ERK pathway (Provenzano et al., 2009).

GEF-H1 overexpression in mouse fibroblasts has been shown to have transforming ability even in the absence of other oncogenes or tumor suppressors (Brecht et al., 2005), and a cell line transformed by GEF-H1 overexpression induces tumor formation in nude mice (Frolov et al., 2003). Consistent with these data, GEF-H1 protein expression is up-regulated in human breast tumors and surrounding

stromal cells up to 4 cm from the primary tumor (Cheng et al., 2008). Of interest, GEF-H1 mRNA and protein expression is down-regulated in FAK-ablated mouse mammary tumors that are not locally invasive and do not metastasize to the lung (Provenzano et al., 2008). A role for GEF-H1 in breast carcinoma metastasis driven by hPTTG1 supports the idea that GEF-H1 may be part of the metastatic cascade (Liao et al., 2011). Consistent with these findings, we find that loss of GEF-H1 expression diminishes cell invasion across a collagen matrix. An interesting aspect of the invasion is that there was significantly less invasion across a dense matrix, although this migration was still inhibited in GEF-H1–knockdown MDA-MB-231 cells. The reason for the diminished migration in a dense matrix may reflect a greater barrier function of a dense matrix or that the matrix has more choices for a cell to move randomly rather than across the Transwell.

In summary, these data demonstrate that microtubule instability in response to increased extracellular matrix stiffness and downstream signaling through GEF-H1 and RhoA is an important mechanism by which breast epithelial cells respond to biomechanical changes in their matrix environment.

MATERIALS AND METHODS
Reagents and antibodies
Type I collagen was purchased from BD Biosciences (Bedford, MA), and all culture media were purchased from Life Technologies (Grand Island, NY). Nocodazole and paclitaxel (Sigma-Aldrich, St. Louis, MO) and the MEK inhibitor UO126 (Promega, Madison, WI) were dissolved in dimethyl sulfoxide (DMSO). Antibodies used were as follows: GEF-H1 (55B6) and RhoA (Cell Signaling, Danvers, MA), α-tubulin (clone B-5-1-2) and acetylated α-tubulin (Sigma-Aldrich), Rho (A-, B-, C-, clone 55; BD Biosciences, San Jose, CA), ACTIVE MAPK and ERK1/2 (Promega, Madison, WI), and glyceraldehyde-3-phosphate dehydrogenase (GAPDH: Santa Cruz Biotechnology, Santa Cruz, CA). Horseradish peroxidase (HRP)–conjugated secondary antibodies were purchased from Jackson ImmunoResearch Laboratories (Westgrove, PA). Bisbenzimide and tetramethylrhodamine isothiocyanate (TRITC)–conjugated phalloidin was purchased from Sigma-Aldrich, and Alexa Fluor secondary antibodies were purchased from Invitrogen (Carlsbad, CA).

shRNA and DNA constructs
Lentiviral nontargeting pLKO.1 vector control, pGIPz vector control, and nine mouse (sequences in pLK0.1: GCAGGAGATTTACAAC-CGAAT, CGACGCTTTATACTTGAGCTT, CCCTCATTTGTCCTAC-ATGTA, TCAGTGACATTCACACACGTT, and sequences in pGIPz: CCGTGAGAACCTTGAAGATTAT, ACCTGTCCGTGGAATCCCTT-ATT, CTCCCTTATTGATGAAGG-TGTA, AAAGAAGCAAGATGT-CATCTAT, ACAGGACATTCCTGAAGAGACA) and five human-specific (pLK0.1 sequences: GCGGCGAATTAAGATGGAGTT, CGAT-GCCCTGTACTTGAGTTT, CGCTCTGTCCATCGAAACTTT, CGTAG-GCAATTAGAGATCGAA, CCCAACCTGCAATGTGACTAT) GEF-H1 shRNAs were purchased from Open Biosystems (Huntsville, AL). Mature sense sequences used to generate GEF-H1–knockdown cell lines were CCGTGAGAACCTTGAAGATTAT (mouse, pGIPz #1),

GCAGGAGATTTACAACCGAAT (mouse, pLK0.1 #2), and CCCA-ACCTGCAATGTGACTAT (human pLK0.1 #5). Human GEF-H1 cDNA was purchased from Open Biosystems and was cloned into pBABE lentiviral GFP expression vector. The resulting construct was confirmed by sequence and expression analysis. GST-tagged Rho(G17A) in the bacterial expression vector pGEX-4T1 was a kind gift from Keith Burridge (University of North Carolina, Chapel Hill, NC).

Cell culture and transfection
NMuMG cells were maintained in high-glucose DMEM containing 0.2 U/ml bovine insulin and 10% fetal bovine serum (FBS). T47D human carcinoma cells were maintained in RPMI 1640 containing 0.2 U/ml bovine insulin and 10% FBS. MDA-MB-231 cells were maintained in low-glucose DMEM containing 10% FBS. All cell lines were incubated at 37°C with 5% CO_2. Cells were stably transfected using FuGENE 6 (Roche Bioscience, Indianapolis, IN) with species-specific GEF-H1 shRNA or pLKO.1 vector control. Phoenix (HEK293) viral packaging cells were transfected with pGIPz-GEF-H1 shRNA, GIPz alone, GFP-tagged GEF-H1, or GFP alone along with 5:1 ratio of pCMV 8.9.1 and VSV-G. At 24 h posttransfection, cells were moved to 30% serum for 48 h. Virus-containing media were collected, mixed with 1:1000 dilution of 1 µg/ml polybrene (Millipore, Billerica, MA), and used to infect target cells (RNAi Consortium, Broad Institute of MIT and Harvard, Cambridge, MA). For overexpressing cell lines, NMuMG cells were infected with lentiviral-packaged, GFP-tagged human GEF-H1 or GFP alone. At 48 h postinfection, cells were selected in 5 µg/ml puromycin, and expression was confirmed by Western blot. For knockdown, NMuMg cells were infected with lentiviral-packaged pGIPz GEF-H1 shRNA #2 or pGIPz alone. At 48–72 h postinfection, cells were seeded into collagen gels for RhoA activity measurements.

Cells were cultured in type I collagen gels as described previously (Wozniak and Keely, 2005). Briefly, gels containing cells were poured with serum-free media plus 5 µg/ml bovine serum albumin (BSA) to control for serum effects into six-well plates and allowed to polymerize for 1 h at 37°C. A 2-ml amount of complete or BSA media was added, and gels were detached from the sides and bottom of the dish (floating). The time at which the gels were rendered floating was considered day and time 0. For drug treatment experiments, gels were pretreated for 30 min with 1 ml of BSA media containing DMSO or 10 µM nocodazole, 10 µM paclitaxel, or 10 µM UO126 and then floated in an additional 1 ml of drug containing BSA media for 2–4 h.

Compliant (low-density) and stiff (high-density) matrix conditions were achieved by altering the concentration of type I collagen in the collagen gel. The concentration of collagen that was considered compliant or stiff was determined experimentally for each cell type based on the ability of the cells to undergo morphological changes and/or their ability to physically contract the collagen gel (Wozniak and Keely, 2005). For T47D cells, 1.3 mg/ml type I collagen was used for compliant and 2.0 mg/ml was used for stiff matrix conditions. For NMuMG and MDA-MB-231 cells, 2.0 mg/ml type I collagen was used for compliant and 4.0 mg/ml was used for stiff matrix conditions (Wozniak et al., 2003; Gehler et al., 2009).

Western blotting and immunofluorescence
Protein expression was assessed by Western blot. Briefly, cells were lysed in Laemmli buffer and boiled for 3 min, and proteins were separated by SDS–PAGE. Proteins were transferred to polyvinylidene fluoride membrane, and membranes were blocked using 3% BSA plus 0.3% Tween-20 in TBS (TBST). Membranes were probed with 1:1000 anti–GEF-H1, 1:1000 anti-Rho, 1:5000 anti-GAPDH, 1:1000 anti–acetylated α-tubulin, 1:1000 anti–α-tubulin, 1:2500 active MAPK, or 1:2500 ERK1/2, followed by incubation with 1:5000 HRP-conjugated secondary antibodies. Proteins were visualized using ECL reagents (Pierce, Rockford, IL).

Localization of GEF-H1, as well as of microtubule and actin organization, in collagen matrices was determined by immunofluorescence similar to that previously described (Wozniak et al., 2003). Briefly, cells in gels were treated with DMSO, 10 µM nocodazole, or 10 µM paclitaxel as described earlier. Gels were fixed in 4% paraformaldehyde, permeabilized in 0.5% Triton X-100, and blocked in 3% BSA. GEF-H1 and acetylated α-tubulin primary antibodies were used at 1:500 and incubated overnight at 4°C. Alexa 488 and 594 secondary antibodies were used at 1:500 and incubated 1 h at room temperature. TRITC-conjugated phalloidin was used at 1:1000 and incubated 1 h at room temperature. Cells were counterstained with bisbenzamide at 1:15,000 for 5 min at room temperature. Fluorescence microscopy was carried out using an Olympus FluoView FV1000 confocal microscope (Olympus, Center Valley, PA) with a 60×/1.42 numerical aperture oil immersion objective. FIJI ImageJ (FIJI Consortium, National Institutes of Health, Bethesda, MD) was used for linear adjustments of brightness and contrast. Actin morphology was determined by observer assessment of randomized photographs for nine cells in each treatment group. Three independent observers assessed the structure and density of cortical actin fibers, and since there were no obvious differences, further quantification was not pursued. Cell proliferation was assessed in control and GEF-H1–knockdown cells by counting 4′,6-diamidino-2-phenylindole–stained nuclei in four fields of view in two gels per condition for each cell line. Data are expressed as an average number of nuclei in each cell line and collagen density.

Microtubule structural quantification
Quantitative analysis of microtubule perturbation was performed using CurveAlign, a specialized Matlab program (MathWorks, Natick, MA) based on the curvelet transform (Candès and Donoho, 1999; Candès et al., 2006). The curvelet transform is an overcomplete nonadaptive representation of an image using a series of energy measurements that range across scale, orientation, and position; the m-term approximation using a curvelet representation outperforms both the Fourier and wavelet representations and is nearly as good as the best adaptive techniques (Candès and Donoho, 1999). CurveAlign outputs a normalized measure of anisotropy based on the distribution of curvelet coefficients generated from each image and was used to quantify the structural differences between the microtubules of cells grown in stiff collagen gels and those of cells grown in compliant collagen gels. CurveAlign can be downloaded at http://loci.wisc.edu/software/curvelet-based-alignment-analysis.

Collagen matrix contraction measurements and morphogenesis
Gel contraction measurements were performed as described previously (Keely et al., 2007). Gels were poured and released in complete media as described. For Rho inhibition, the gels were released into media containing 50% glycerol (vehicle control) or 1 µg/ml cell-permeable exoenzyme C3 transferase. The time at which the gels were rendered floating was considered day 0. Gel diameter was measured every day for 10 d. For matrix contraction, day 10 gels were lysed in 2× RIPA buffer (50 mM Tris, pH 7.4, 150 mM NaCl, 2 mM EDTA, 2 mM NaF, 2 mM NaVO$_4$, 2% NP-40, 0.5% sodium deoxycholate) as described previously for total protein concentration determined by

amido black staining (Sheffield et al., 1987). Data were presented as total contraction (in millimeters) over time or as day 10 contraction normalized to total protein. For morphogenesis, gels that had been incubated for 10 d were fixed with 4% paraformaldehyde. Phase contrast microscopy was carried out using a Nikon TE300 inverted microscope (Nikon, Melville, NY) equipped with a Cool-SNAP fx CCD camera (Tucson, AZ). Images were acquired using SlideBook, version 4.2 (Intelligent Imaging Innovations, Denver, CO), and processed using Adobe Photoshop CS2 (Adobe Systems, San Jose, CA).

RhoA activity assays

RhoA activity was measured using a Rho-GLISA kit (Cytoskeleton, Denver, CO) and normalized to total RhoA determined by Western blot analysis as described previously (Keely et al., 2007). Briefly, 1×10^6 cells were cultured in gels floated in BSA media for 2 h. Gels were lysed on ice in 400 μl of lysis buffer provided. After centrifugation, 75 μl of supernatant was assayed in a plate format following the G-LISA protocol, and 60 μl of supernatant was loaded on an SDS–PAGE gel for Western blot analysis of total RhoA levels. Active RhoA detected by chemiluminescence was normalized to total RhoA determined by densitometry using Image J (National Institutes of Health, Bethesda, MD).

Affinity precipitation of activated GEFs

Active GEF-H1 was affinity precipitated from cell lysates using the Rho(G17A) mutant, which cannot bind nucleotide and therefore has high affinity for activated RhoA GEFs (Garcia-Mata et al., 2006). A total of 5×10^6 cells were cultured in gels poured with BSA media and allowed to polymerize for 1 h. Gels were released and floated in BSA media for an additional 2 h and then lysed on ice in 2× RIPA buffer. After centrifugation, cell lysates were incubated with GST or GST-Rho(G17A) in the presence of glutathione-S Sepharose beads (GE Healthcare, Piscataway, NJ) for 2 h at 4°C. Activated GEF-H1 in the precipitates and total GEF-H1 in the cell lysates was detected by Western blot as described. Active and total GEF-H1 were quantified by densitometry as described, and the amount of active GEF-H1 was normalized to total GEF-H1 for each sample.

3D cell migration and invasion in vitro and in vivo tumorigenesis

To assess cell migration and invasion in 3D cultures, 2×10^5 NMuMG or 3×10^5 MDA-MB-231 cells were cultured in compliant and stiff collagen matrices poured with BSA media in a Transwell insert with 8- or 12-μm pore-size filter membrane, respectively (Corning, Corning, NY) and allowed to polymerize for 1 h. Once polymerized, 650 μl of full serum media or BSA media as a serum control was filled in the lower chamber, and cells were allowed 24 h to migrate and transverse the Transwell filter. Cell migration and invasion for each condition were determined according to manufacturer's recommendations. Briefly, gels and media were removed from the tops and bottoms of the insert and the wells were rinsed with phosphate-buffered saline. Cell dissociation solution (Trevigen, Helgerman, CT) containing 2 μg/ml of Calcein AM live-cell stain (Molecular Probes, Eugene, OR) was added to each well so that the bottom of the Transwell insert was contacting the liquid but not submerged and incubated at 37°C for 60 min with occasional gentle agitation. After incubation, the bottom of the Transwell filter was gently rinsed, and the number of migrated cells was determined by fluorescence with 485-nm excitation and 520-nm emission. Data are presented as the percentage of migrated cells for each condition.

Statistical analysis

All statistical analysis was completed using the program GraphPad Prism 4 (GraphPad Software, La Jolla, CA). For direct comparisons of two conditions, a Student's t test was preformed. For comparisons of multiple parameters an analysis of variance was completed, followed by a Bonferroni post hoc test. Error bars are represented as SEM.

REFERENCES

Aijaz S, D'Atri F, Citi S, Balda MS, Matter K (2005). Binding of GEF-H1 to the tight junction-associated adaptor cingulin results in inhibition of Rho signaling and G1/S phase transition. Dev Cell 8, 777–786.

Bakal CJ, Finan D, LaRose J, Wells CD, Gish G, Kulkarni S, DeSepulveda P, Wilde A, Rottapel R (2005). The Rho GTP exchange factor Lfc promotes spindle assembly in early mitosis. Proc Natl Acad Sci USA 102, 9529–9534.

Benais-Pont G, Punn A, Flores-Maldonado C, Eckert J, Raposo G, Fleming TP, Cereijido M, Balda MS, Matter K (2003). Identification of a tight junction-associated guanine nucleotide exchange factor that activates Rho and regulates paracellular permeability. J Cell Biol 160, 729–740.

Birkenfeld J, Nalbant P, Bohl BP, Pertz O, Hahn KM, Bokoch GM (2007). GEF-H1 modulates localized RhoA activation during cytokinesis under the control of mitotic kinases. Dev Cell 12, 699–712.

Birkenfeld J, Nalbant P, Yoon SH, Bokoch GM (2008). Cellular functions of GEF-H1, a microtubule-regulated Rho-GEF: is altered GEF-H1 activity a crucial determinant of disease pathogenesis? Trends Cell Biol 18, 210–219.

Birukova AA, Fu P, Xing J, Yakubov B, Cokic I, Birukov KG (2010). Mechanotransduction by GEF-H1 as a novel mechanism of ventilator-induced vascular endothelial permeability. Am J Physiol Lung Cell Mol Physiol 298, L837–L848.

Boyd NF, Lockwood GA, Martin LJ, Knight JA, Byng JW, Yaffe MJ, Tritchler DL (1998). Mammographic densities and breast cancer risk. Breast Dis 10, 113–126.

Brecht M, Steenvoorden AC, Collard JG, Luf S, Erz D, Bartram CR, Janssen JW (2005). Activation of gef-h1, a guanine nucleotide exchange factor for RhoA, by DNA transfection. Int J Cancer 113, 533–540.

Callow MG, Zozulya S, Gishizky ML, Jallal B, Smeal T (2005). PAK4 mediates morphological changes through the regulation of GEF-H1. J Cell Sci 118, 1861–1872.

Candès E, Demanet L, Donoho D, Lexing Ying (2006). Fast discrete curvelet transforms. Multiscale Modeling Simulation 5, 861–899.

Candès E, Donoho D (1999). Curvelets—a surprisingly effective nonadaptive representation for objects with edges. In Curves and Surface Fitting: Saint-Malo 1999, eds. A Cohen, C Rabut, L Schumaker, Nashville, TN: Vanderbilt University Press, 105–120.

Chang YC, Nalbant P, Birkenfeld J, Chang ZF, Bokoch GM (2008). GEF-H1 couples nocodazole-induced microtubule disassembly to cell contractility via RhoA. Mol Biol Cell 19, 2147–2153.

Cheng AS et al. (2008). Epithelial progeny of estrogen-exposed breast progenitor cells display a cancer-like methylome. Cancer Res 68, 1786–1796.

Dubash AD, Wennerberg K, Garcia-Mata R, Menold MM, Arthur WT, Burridge K (2007). A novel role for Lsc/p115 RhoGEF and LARG in

regulating RhoA activity downstream of adhesion to fibronectin. J Cell Sci 120, 3989–3998.

Frolov A, Chahwan S, Ochs M, Arnoletti JP, Pan ZZ, Favorova O, Fletcher J, von Mehren M, Eisenberg B, Godwin AK (2003). Response markers and the molecular mechanisms of action of Gleevec in gastrointestinal stromal tumors. Mol Cancer Ther 2, 699–709.

Fujishiro SH, Tanimura S, Mure S, Kashimoto Y, Watanabe K, Kohno M (2008). ERK1/2 phosphorylate GEF-H1 to enhance its guanine nucleotide exchange activity toward RhoA. Biochem Biophys Res Commun 368, 162–167.

Garcia-Mata R, Wennerberg K, Arthur WT, Noren NK, Ellerbroek SM, Burridge K (2006). Analysis of activated GAPs and GEFs in cell lysates. Methods Enzymol 406, 425–437.

Gehler S, Baldassarre M, Lad Y, Leight JL, Wozniak MA, Riching KM, Eliceiri KW, Weaver VM, Calderwood DA, Keely PJ (2009). Filamin A-beta1 integrin complex tunes epithelial cell response to matrix tension. Mol Biol Cell 20, 3224–3238.

Guillemot L, Paschoud S, Jond L, Foglia A, Citi S (2008). Paracingulin regulates the activity of Rac1 and RhoA GTPases by recruiting Tiam1 and GEF-H1 to epithelial junctions. Mol Biol Cell 19, 4442–4453.

Guilluy C, Swaminathan V, Garcia-Mata R, O'Brien ET, Superfine R, Burridge K (2011). The Rho GEFs LARG and GEF-H1 regulate the mechanical response to force on integrins. Nat Cell Biol 13, 722–727.

Guo YP, Martin LJ, Hanna W, Banerjee D, Miller N, Fishell E, Khokha R, Boyd NF (2001). Growth factors and stromal matrix proteins associated with mammographic densities. Cancer Epidemiol Biomarkers Prev 10, 243–248.

Heasman SJ, Carlin LM, Cox S, Ng T, Ridley AJ (2010). Coordinated RhoA signaling at the leading edge and uropod is required for T cell transendothelial migration. J Cell Biol 190, 553–563.

Ingber DE (2003). Tensegrity II. How structural networks influence cellular information processing networks. J Cell Sci 116, 1397–1408.

Kaverina I, Krylyshkina O, Beningo K, Anderson K, Wang YL, Small JV (2002). Tensile stress stimulates microtubule outgrowth in living cells. J Cell Sci 115, 2283–2291.

Keely PJ, Conklin MW, Gehler S, Ponik SM, Provenzano PP (2007). Investigating integrin regulation and signaling events in three-dimensional systems. Methods Enzymol 426, 27–45.

Krendel M, Zenke FT, Bokoch GM (2002). Nucleotide exchange factor GEF-H1 mediates cross-talk between microtubules and the actin cytoskeleton. Nat Cell Biol 4, 294–301.

Liao YC, Ruan JW, Lua I, Li MH, Chen WL, Wang JR, Kao RH, Chen JH (2011). Overexpressed hPTTG1 promotes breast cancer cell invasion and metastasis by regulating GEF-H1/RhoA signalling. Oncogene, doi: 10.1038/onc.2011.476.

Liu BP, Chrzanowska-Wodnicka M, Burridge K (1998). Microtubule depolymerization induces stress fibers, focal adhesions, and DNA synthesis via the GTP-binding protein Rho. Cell Adhes Commun 5, 249–255.

Mialhe A et al. (2001). Tubulin detyrosination is a frequent occurrence in breast cancers of poor prognosis. Cancer Res 61, 5024–5027.

Myers KA, Applegate KT, Danuser G, Fischer RS, Waterman CM (2011). Distinct ECM mechanosensing pathways regulate microtubule dynamics to control endothelial cell branching morphogenesis. J Cell Biol 192, 321–334.

Nalbant P, Chang YC, Birkenfeld J, Chang ZF, Bokoch GM (2009). Guanine nucleotide exchange factor-H1 regulates cell migration via localized activation of RhoA at the leading edge. Mol Biol Cell 20, 4070–4082.

Nie M, Aijaz S, Leefa Chong San IV, Balda MS, Matter K (2009). The Y-box factor ZONAB/DbpA associates with GEF-H1/Lfc and mediates Rho-stimulated transcription. EMBO Rep 10, 1125–1131.

Palazzo AF, Gundersen GG (2002). Microtubule-actin cross-talk at focal adhesions. Sci STKE 2002, pe31.

Paszek MJ, Weaver VM (2004). The tension mounts: mechanics meets morphogenesis and malignancy. J Mammary Gland Biol Neoplasia 9, 325–342.

Provenzano PP, Inman DR, Eliceiri KW, Beggs HE, Keely PJ (2008). Mammary epithelial-specific disruption of focal adhesion kinase retards tumor formation and metastasis in a transgenic mouse model of human breast cancer. Am J Pathol 173, 1551–1565.

Provenzano PP, Inman DR, Eliceiri KW, Keely PJ (2009). Matrix density-induced mechanoregulation of breast cell phenotype, signaling and gene expression through a FAK-ERK linkage. Oncogene 28, 4326–4343.

Putnam AJ, Cunningham JJ, Pillemer BB, Mooney DJ (2003). External mechanical strain regulates membrane targeting of Rho GTPases by controlling microtubule assembly. Am J Physiol Cell Physiol 284, C627–639.

Ren Y, Li R, Zheng Y, Busch H (1998). Cloning and characterization of GEF-H1, a microtubule-associated guanine nucleotide exchange factor for Rac and Rho GTPases. J Biol Chem 273, 34954–34960.

Rhee S, Jiang H, Ho CH, Grinnell F (2007). Microtubule function in fibroblast spreading is modulated according to the tension state of cell-matrix interactions. Proc Natl Acad Sci USA 104, 5425–5430.

Roeder BA, Kokini K, Sturgis JE, Robinson JP, Voytik-Harbin SL (2002). Tensile mechanical properties of three-dimensional type I collagen extracellular matrices with varied microstructure. J Biomech Eng 124, 214–222.

Sheffield JB, Graff D, Li HP (1987). A solid-phase method for the quantitation of protein in the presence of sodium dodecyl sulfate and other interfering substances. Anal Biochem 166, 49–54.

Small JV, Kaverina I (2003). Microtubules meet substrate adhesions to arrange cell polarity. Curr Opin Cell Biol 15, 40–47.

Stamenovic D, Mijailovich SM, Tolic-Norrelykke IM, Chen J, Wang N (2002). Cell prestress. II. Contribution of microtubules. Am J Physiol Cell Physiol 282, C617–C624.

Tonami K, Kurihara Y, Arima S, Nishiyama K, Uchijima Y, Asano T, Sorimachi H, Kurihara H (2011). Calpain-6, a microtubule-stabilizing protein, regulates Rac1 activity and cell motility through interaction with GEF-H1. J Cell Sci 124, 1214–1223.

Tsapara A, Luthert P, Greenwood J, Hill CS, Matter K, Balda MS (2010). The RhoA activator GEF-H1/Lfc is a transforming growth factor-beta target gene and effector that regulates alpha-smooth muscle actin expression and cell migration. Mol Biol Cell 21, 860–870.

Ursin G, Hovanessian-Larsen L, Parisky YR, Pike MC, Wu AH (2005). Greatly increased occurrence of breast cancers in areas of mammographically dense tissue. Breast Cancer Res 7, R605–R608.

Waheed F, Speight P, Kawai G, Dan Q, Kapus A, Szaszi K (2010). Extracellular signal-regulated kinase and GEF-H1 mediate depolarization-induced Rho activation and paracellular permeability increase. Am J Physiol Cell Physiol 298, C1376–C1387.

Wozniak MA, Desai R, Solski PA, Der CJ, Keely PJ (2003). ROCK-generated contractility regulates breast epithelial cell differentiation in response to the physical properties of a three-dimensional collagen matrix. J Cell Biol 163, 583–595.

Wozniak MA, Keely PJ (2005). Use of three-dimensional collagen gels to study mechanotransduction in T47D breast epithelial cells. Biol Proced Online 7, 144–161.

Zenke FT, Krendel M, DerMardirossian C, King CC, Bohl BP, Bokoch GM (2004). p21-activated kinase 1 phosphorylates and regulates 14-3-3 binding to GEF-H1, a microtubule-localized Rho exchange factor. J Biol Chem 279, 18392–18400.